Low-energy collisions of O^{5+} ions with He atoms: Single-electron capture, projectile excitation, and transfer excitation and ionization

N. Shimakura,[1,2] S. Yamada,[1] and S. Suzuki[2]
[1]*Department of Chemistry, Faculty of Science, Niigata University, Niigata 950-21, Japan*
[2]*Graduate School of Science and Technology, Niigata University, Niigata 950-21, Japan*

M. Kimura
Argonne National Laboratory, Argonne, Illinois 60439
and Department of Physics, Rice University, Houston, Texas 77251
(Received 24 October 1994)

A theoretical study of various inelastic processes resulting from collisions of O^{5+} ions with He atoms is carried out by a semiclassical molecular-orbital expansion method with the inclusion of electron translation factors at collision energies of 60 eV/u to 15 keV/u. In addition to the single-electron-capture process, projectile excitation and transfer excitation and ionization processes are also studied, and the corresponding cross sections are determined. Dominant processes are found to be a single-electron capture to the $O^{4+}(2s3s)$ and $O^{4+}(2s3p)$ states. Other channels are found to make weak but non-negligible contributions. All processes proceed on the outgoing part of the collision, after the transitions from the initial channel to the single-electron-capture channels are completed. Hence, direct processes to projectile excitation and transfer excitation are nearly negligible. The agreement of the present calculation for single-electron capture with measurements is very good.

PACS number(s): 34.70.+e, 34.50.−s, 39.10.+j

I. INTRODUCTION

The various processes in collisions of multiply charged ions with atoms are important not only in basic atomic collision physics but also for applications in many fields of physics. Many theoretical studies based on close coupling and perturbative methods have been performed on one-electron systems over the last 20 years, but studies of systems with more than two electrons are rare as yet.

In previous papers, we reported on detailed studies of electron capture in two active-electron systems, namely the $O^{6+}+He$ [1] and $O^{5+}+H$ [2] systems, where $O^{6+}(1s^2)$ core electrons were considered to be inert and were treated by a pseudopotential. In this paper, the cross sections for various inelastic processes in collisions of O^{5+} ions with He atoms are reported at collision energies from 62.5 eV/u to 11.3 keV/u. In this system, in addition to pure single-electron capture (SEC), other processes are found to be simultaneously possible. These processes include single-electron capture with the simultaneous excitation and ionization of another electron [transfer excitation and ionization, a process sometimes called resonant transfer excitation (RTE) for projectile electron excitation], electron excitation in the projectile [projectile excitation (PE)] or in the target, and two-electron capture. However, because two-electron capture is known to be a secondary process, we consider only the following three processes in the present model:

Single-electron capture,

$$O^{5+}(1s^2 2s)+He \rightarrow O^{4+}(1s^2 2snl)+He^+ ; \quad (1a)$$

projectile excitation,

$$O^{5+}(1s^2 2s)+He \rightarrow O^{5+}(1s^2 nl)+He ; \quad (1b)$$

and single-electron capture with excitation of the projectile electron,

$$O^{5+}(1s^2 2s)+He \rightarrow O^{4+}(1s^2 nln'l')+He^+ . \quad (1c)$$

In addition, we performed a limited study of the following ionization processes:

Target ionization,

$$O^{5+}(1s^2 2s)+He \rightarrow O^{5+}(1s^2 nl)+He^+ +1e ; \quad (1d)$$

and projectile electron loss,

$$O^{5+}(1s^2 2s)+He \rightarrow O^{6+}(1s^2)+He+1e . \quad (1e)$$

Different pathways leading to the three processes concerned were allowed. We allowed (i) a simple one-step pathway involving an electron from a target or on a projectile (for SEC and PE) and (ii) a two-step process in which a projectile electron was first excited and then a target electron was transferred to the hole (for SEC), or a target electron was transferred to an excited orbital of the projectile and an inner electron of the projectile was transferred back to the target (PE), or a target electron was captured into the nl state while a projectile electron was excited into the $n'l'$ state or vice versa (for RTE). These two different pathways are expected to interfere; they were examined to identify the signature of the dynamics. As a theoretical model, we use a molecular-orbital (MO) expansion method modified by atomic-type electron translation factors (ETF's) within a semiclassical representation. Coupled equations with a straight-line trajectory are solved numerically to extract scattering

amplitudes.

Several measurements exist, for comparison with our calculated results. Gardner *et al.* [3] measured the cross sections for SEC in the $O^{5+}+He$ system at a collision energy of 2.5 keV/u. At energies of 0.47, 0.63, and 0.78 keV/u, Iwai *et al.* [4] reported cross sections for SEC for the same system. Distributions of the captured electrons over the final-state quantum numbers n and l in the $O^{4+}(2snl)$ state were measured by Kimura *et al.* [5] with a beam spectroscopy method at energy $E=0.326$ keV/u. Hoekstra, de Heer, and Winter [6] measured double-electron capture, simultaneous SEC with target excitation, and simple SEC at collision energies of 0.5–6 keV/u. Their results show that the cross sections for SEC are about 20 times larger than that for double-electron capture, with the cross section for simultaneous SEC and target excitation being still smaller. Hoekstra, de Heer, and Winter [6] also noted that double-electron capture into bound states is considerably more important than that into autoionizing states. If the charge of a projectile ion becomes larger than 5, double-electron capture into autoionizing states gradually becomes dominant over that into bound states. The angular distribution of the projectile as a result of electron capture was measured at energies ranging from 0.5 to 1 keV/u by Waggoner *et al.* [7]. At very low collision energy $E=0.03$ keV/u, Bangsgaard *et al.* [8] performed energy-gain measurements for SEC in the same system.

At collision energies above 50 keV/u, which the present study does not cover, measurements of cross sections for SEC in the $O^{5+}+He$ collision system were obtained in the region of hundreds of keV/u by MacDonald and Martin [9] and Knudsen, Haugen, and Hvelplund [10], at 30–100 keV/u by Bayfield *et al.* [11], and at 1 MeV/u by Boman, Bernstein, and Tanis [12]. The contribution of transfer ionization to the total electron capture was measured by Tanis *et al.* [13] for the same system at energies of 0.5–1.5 MeV/u. Swenson *et al.* [14] presented evidence for resonant transfer and excitation in this collision system at collision energies of 0.3–2 MeV/u, by using the technique of high-resolution Auger-electron spectroscopy. Zouros, Lee, and Richard [15] experimentally identified the role of electron-electron interaction for projectile $1s$-$2p$ excitation above 0.75 MeV/u.

Only one theoretical attempt has considered this system. In this study, the cross sections of electron capture and ionization were calculated at collision energies above 50 keV/u based on the classical trajectory Monte Carlo (CTMC) method by Janev and McDowell [16]. No theoretical study has been reported in the present energy region.

II. SUMMARY OF THEORY

Because the details of the method employed in this paper were reported previously [2,17,18], only the outline of the basic technique and the specific information used for this calculation are shown.

A. Molecular states

The calculations of the molecular electronic states were performed by using a modified valence-bond configuration interaction method. The $(OHe)^{5+}$ system has five electrons, but we treated the $2s$ electron on the O^{5+} ion and one of the two $1s$ electrons on He explicitly as active electrons. Interactions between these active electrons, the $1s^2$ core in O^{5+} and another $1s$ electron on He, were replaced by a model potential. Our model potential for the O^{6+} ion has a Gaussian-type form,

$$V(\vec{r}_A)=\sum_{l,m} V_l(r_A)|Y_{lm}\rangle\langle Y_{lm}| \tag{2a}$$

and

$$V_l(r_A)=A_l\exp(-\xi_l r_A^2)-\frac{\alpha_d}{2(r_A^2+d^2)^2} -\frac{\alpha_q}{2(r_A^2+d^2)^3}+\frac{6}{r_A}\ . \tag{2b}$$

Here $|Y_{lm}\rangle$ are the spherical harmonics and r_A is the distance of the active electron from the projectile O^{6+} ion. All parameters, A_l, ξ_l, α_d, α_q, and d, in Eqs. (2) are taken from our previous work [2] and the review by Dalgarno [19]. On the other hand, the model potential for the He^+ ion has a Hellman-type form and is taken from the paper by Ermolaev [20],

$$V_{He^+}=-\frac{1}{r_B}-\frac{(Z_B-1)e^{-\beta r_B}}{r_B}\ , \tag{3}$$

where parameters are given as $Z_B=2$ and $\beta=2.125$, and r_B denotes the electronic coordinate centered at the He nucleus. Because the simultaneous two-electron transition on He is a weak process, this approximation is reasonable, as discussed by Jain, Lin, and Fritsch [21]. We expand the adiabatic wave function for discrete states in terms of Slater determinants. Slater-type orbitals (STO's) used as basis sets consisted of 54 STO's for O^{5+} and O^{4+} ions and five STO's for He atoms. The orbital exponents for the O^{5+} and O^{4+} ions were taken from our previous work [2], in which we employed the different values for the triplet and singlet formations. The orbital exponents of the He atoms were taken from the paper by Opradolce, Valiron, and McCarroll [22]. The accuracy of the present molecular calculation with respect to the spectroscopic energies [23] is better than 0.2% for all states.

Continuum electronic states for single ionization are obtained in the fixed-nuclei static-exchange approximation to elastic electronic scattering from the (OHe^{6+}) molecular ion [24] in conjunction with these pseudopotentials for the O^{6+} and He electrons described above. For generating continuum states, we include the $(OHe)^{6+}$ molecular ions whose asymptotic forms converge to $O^{6+}+He+1e$ and $O^{5+}+He^{+}+1e$ channels. Thus, we distinguish ionization and electron-loss processes. A discretized-energy sampling procedure, based on the Gaussian quadrature, was used to select continuum states for the molecular expansion method. All wave functions were appropriately orthogonalized by the Schmidt procedure.

B. Collision dynamics

A semiclassical approach is used at collision energies of 62.5 eV/u to 11.3 keV/u. The total wave function is expanded in terms of products of an electronic wave function and an ETF, with the expansion coefficients being a scattering amplitude. Substituting this total wave function into the time-dependent Schrödinger equation yields a set of linear first-order coupled equations, which are solved numerically subject to the initial condition, that is, $a_i(t \to -\infty)=\delta_{ij}$, under the assumption of straight-line trajectories for heavy-particle motion. The transition probability to the mth state at $t \to +\infty$, defined as a function of collision energy E and impact parameter b, is obtained as a square of the scattering amplitude. The total cross section for the transition to the mth state is given by an integration of impact-parameter-weighted probability over impact parameter.

Included in the close-coupling calculation are 22 discrete MO's, including (both for the triplet and singlet formations): (i) the initial $O^{5+}+He$ channel; (ii) the SEC $O^{4+}(2snl)+He^{+}$ channels, $nl=3s$ (Σ), $3p$ (Σ and Π), $3d$ (Σ and Π), $4s$ (Σ), $4p$ (Σ and Π); (iii) the PE $O^{5+}(2p)+He$ Σ and Π channels, and (iv) the RTE $O^{4+}(nln'l')+He^{+}$ channels, $nln'l'=2p3s\,P$ (Σ and Π), $2p3p\,D$ (Σ and Π), $2p3p\,S$ (Σ), $2p3p\,P$ (Π), $2p3d\,F$ (Σ and Π), $2p3d\,D$ (Π), and $2p3d\,P$ (Σ and Π). For continuum MO's, 12–18 discretized continuum states are considered for projectile ionization (electron loss) and target ionization. (The energy mesh size is 0.1 for continuum energy ε from 0 to 1 a.u. above the ionization threshold and then 0.2 for $\varepsilon > 1$ a.u.) The primary reason for including these continuum states is to test the convergence of the results for SEC and RTE. However, even though these results are not fully converged, they provide some insight into the mechanism of ionization. We will discuss this aspect in some detail in a later section.

III. RESULTS

A. Adiabatic potentials and couplings

The calculated potential energies for triplet formation in the $(OHe)^{5+}$ system are presented in Fig. 1(a). For simplicity, the Σ states and only one Π state relevant to the present discussion are included. Two potential curves, corresponding to the initial and PE channels, can be diabatically connected with a nearly constant potential value, because the dominant interaction for these channels is a polarization interaction between an ion and a neutral atom. Other potentials show a typical strong Coulomb repulsion that intersects the potential of the former diabatic channel at intermediate R, resulting in a series of avoided crossings. The locations of some avoided crossings and their energy splittings are summarized in Table I. The most important avoided crossings are those between the initial and the SEC channels at R_1, R_2, and R_3. Asymptotically, the initial 4Σ channel has electronic energy between those of the 9Σ [$O^{4+}(2p3d\,P)$] and 10Σ [$O^{4+}(2s4s)$] states; therefore, it has (avoided) crossings with the 5Σ, 6Σ, 7Σ, 8Σ, and 9Σ states at larger internuclear distances, beyond 10 a.u. However, because the energy splittings between the initial and these five Σ channels at the avoided crossings are very small, the avoided crossings can be treated diabatically. (The largest energy splitting is that between the initial and $O^{4+}(2p3s\,P)$ channels, with a magnitude of less than 5×10^{-6} a.u. both for the triplet and singlet formations.) Our test scattering calculations using both the adiabatic and diabatic representations for these crossings gave nearly identical results, supporting the correctness of this treatment. This characteristic is very important in determining the dynamics, because it indicates that all reac-

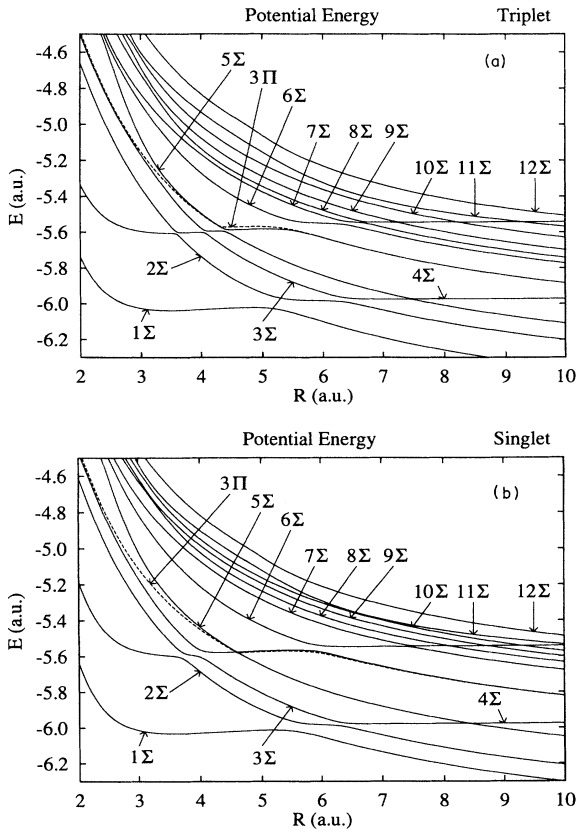

FIG. 1. (a) Adiabatic potentials for the triplet $(OHe)^{5+}$ formation. Twelve Σ states and only one Π state (the most important π state) are shown. 1Σ, $O^{4+}(2s3s)+He^{+}$; 2Σ and 1Π, $O^{4+}(2s3p\,P)+He^{+}$; 3Σ and 2Π, $O^{4+}(2s3d\,D)+He^{+}$; 4Σ, $O^{5+}(2s)+He$; 5Σ and 3Π, $O^{4+}(2p3s\,P)+He^{+}$, 6Σ and 4Π, $O^{4+}(2p3p\,D)+He^{+}$; 7Σ, $O^{4+}(2p3p\,S)+He^{+}$; 5Π, $O^{4+}(2p3p\,P)+He^{+}$; 8Σ and 6Π, $O^{4+}(2p3d\,F)+He^{+}$; 7Π, $O^{4+}(2p3d\,D)+He^{+}$; 9Σ and 8Π, $O^{4+}(2p3d\,P)+He^{+}$; 10Σ, $O^{4+}(2s4s\,S)+He^{+}$; 11Σ and 9Π, $O^{5+}(2p)+He^{+}$; 12Σ and 10Π, $O^{4+}(2s4p\,P)+He^{+}$. (b) Adiabatic potentials for the singlet $(OHe)^{5+}$ formation. Twelve Σ states and only one Π state (the most important π state) are shown. 1Σ, $O^{4+}(2s3s)+He^{+}$; 2Σ and 1Π, $O^{4+}(2s3p\,P)+He^{+}$; 3Σ and 2Π, $O^{4+}(2s3d\,D)+He^{+}$; 4Σ, $O^{5+}(2s)+$ He; 5Σ and 3Π, $O^{4+}(2p3s\,P)+He^{+}$; 6Σ and 4Π, $O^{4+}(2p3p\,D)+He^{+}$; 7Σ, $O^{4+}(2p3p\,S)+He^{+}$; 5Π, $O^{4+}(2p3p\,P)+He^{+}$; 8Σ and 6Π, $O^{4+}(2p3d\,F)+He^{+}$; 7Π, $O^{4+}(2p3d\,D)+He^{+}$; 9Σ and 8Π, $O^{4+}(2p3d\,P)+He^{+}$; 10Σ, $O^{4+}(2s4s\,S)+He^{+}$; 11Σ and 9Π, $O^{5+}(2p)+He^{+}$; 12Σ and 10Π, $O^{4+}(2s4p\,P)+He^{+}$.

TABLE I. Locations of avoided crossings and corresponding energy splittings.

	Triplet		Singlet	
Label	Location (a.u.)	Splitting (a.u.)	Location (a.u.)	Splitting (a.u.)
	Avoided crossings between initial and single-electron capture			
R_1	5.3	6.5×10^{-2}	5.6	5.0×10^{-2}
R_2	6.4	2.4×10^{-2}	6.4	2.0×10^{-2}
R_3	7.5	4.3×10^{-3}	8.4	2.0×10^{-3}
	Avoided crossings between single-electron capture and projectile excitation			
R_4	3.6	1.4×10^{-2}	3.7	3.5×10^{-2}
R_5	4.1	1.4×10^{-2}	4.0	4.0×10^{-2}
R_6	4.4	1.4×10^{-2}	4.6	2.3×10^{-3}
R_7	5.5	5.6×10^{-2}	6.0	4.0×10^{-2}
R_8	6.4	1.9×10^{-2}	7.5	7.0×10^{-3}
R_9	6.7	7.4×10^{-3}	8.1	1.6×10^{-3}

tions occur after the transitions to the SEC channels from the initial channel are completed. The flux transferred to the SEC channels may be successively passed on to the PE channel at the avoided crossings at R_4, R_5, and R_6, and it is finally distributed among the RTE channels at the avoided crossings at R_7 and at larger internuclear distances as the projectile recedes.

Figure 1(b) shows the potential-energy curves for singlet formation. The lowest Σ state $[O^{4+}(2s^2)+He^+]$ is not included because it lies far below the other channels and, in fact, plays no role in the dynamics at the collision energies studied here. General features of the potential energies for singlet formation are similar to those observed for triplet formation. However, the positions of the avoided crossing for singlet formation are slightly larger than those for triplet formation, except at R_2 and R_5. This is because the asymptotic electronic energies of the SEC and RTE channels for singlet formation are slightly higher than those for triplet formation.

All combinations of radial and rotational coupling matrix elements necessary to solve the coupled equations were calculated. Briefly, the peak at R_3 for singlet formation was found to be larger and sharper than that for triplet formation. The peak at R_1 is also slightly larger in singlet formation than in triplet formation.

B. The SEC and RTE processes

1. Total cross sections

a. Triplet. Figure 2(a) shows the total cross sections for the SEC channels for $O^{4+}(2s3l)$ and $O^{4+}(2s4l)$ and the RTE channels for triplet formation. The sum obtained by adding these three cross sections is also shown. The cross sections for SEC for $O^{4+}(2s3l)$ are dominant and almost independent of collision energy, with a slightly decreasing trend at larger collision energies. In contrast, the RTE channel has an oscillatory structure with

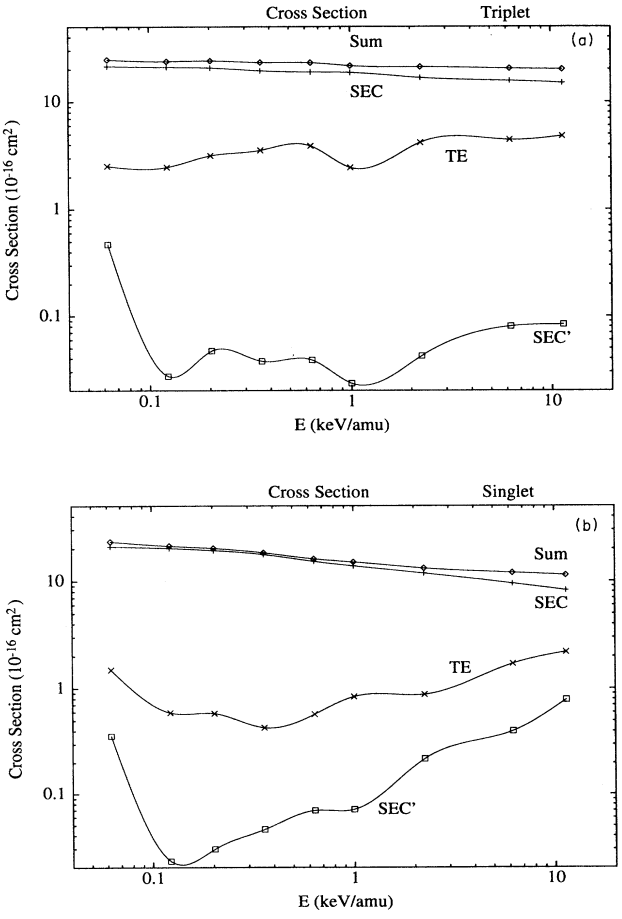

FIG. 2. Cross sections for single-electron capture (SEC) [$-+-$ for $O^{4+}(2s3l)$ labeled as the SEC and $-\square-$ for $O^{4+}(2s4l)$ labeled as the SEC', respectively] and transfer excitation (TE) ($-\times-$) along with the sum ($-\diamond-$) of these three processes for the (a) triplet and (b) singlet manifolds, respectively.

an overall increase with energy. The SEC channel into $O^{4+}(2s4l)$ is small above 0.1 keV/u and has oscillatory structures that are similar in phase to those in the RTE channel. This suggests that the SEC channel into $O^{4+}(2s4l)$ is fed mainly through the RTE channel at the collision energy studied here. The $O^{4+}(2s4l)$ SEC potentials lie close to that of the $O^{5+}(2p)$ PE channel. Hence, these channels are expected to interact strongly with the PE channel, as shown later. The increase in the SEC channel for $O^{4+}(2s4l)$ below 0.1 keV/u is due to the increasing effectiveness of curve crossings between the initial channel and those leading to $O^{4+}(2s4l)$ channels in regions of large R.

b. Singlet. The total cross sections of the SEC and RTE channels for the singlet formation are shown in Fig. 2(b) along with the sum of these cross sections. The SEC channel is again dominant. With increasing collision energy, SEC decreases, while the RTE increases slowly. Oscillatory structures in the RTE and SEC channels for $O^{4+}(2s4l)$ are similar to those seen for triplet formation. However, here the oscillatory patterns are out of phase, suggesting strong coupling between the two channels.

The study of time evolution shows that for the SEC, electron transfer into a hole (a two-step process as discussed in Sec. I) is found to be negligibly small. For the RTE, two contributions and their interference, i.e., target-electron capture into the (nl) state and projectile-electron excitation into the (nl) state, possess the same order in the velocity dependence because of the indistinguishability of the electrons involved, hence allowing the probability of a somewhat more complex behavior due to the interplay of these processes as a function of a collision energy and, thus, may lead to more structures. However, our study of collision history implies that single-electron capture into a higher excited level ($3l$ with $2s$ projectile electron) first takes place at an earlier time followed by a projectile-electron excitation to $2s \rightarrow 2p$, forming $2p3l$ at a later time. Therefore, the process that corresponds to the projectile-electron excitation to a higher state followed by electron transfer into a lower-excited state ($2p$) is a weak process, somewhat weakening an interference between these processes.

2. *Comparison with experimental SEC*

Figure 3 displays the calculated total cross sections for the SEC for the triplet and singlet formations and for their statistical weighted ones along with measurements [3,4,6]. The calculated results for the triplet formation are slightly larger than most of the experiments and the singlet formation. All experimental data show weak energy dependence in the present energy region. The present cross sections, obtained by summing the triplet and singlet formations, are in good agreement with all the experiments within error bars.

3. *Partial distributions of the SEC*

The calculated partial (n,l) cross sections for the SEC process for the triplet and singlet formations are shown in Figs. 4(a) and 4(b), respectively. Capture into the $O^{4+}(2s3s)$ state and capture into the $O^{4+}(2s3p)$ state are

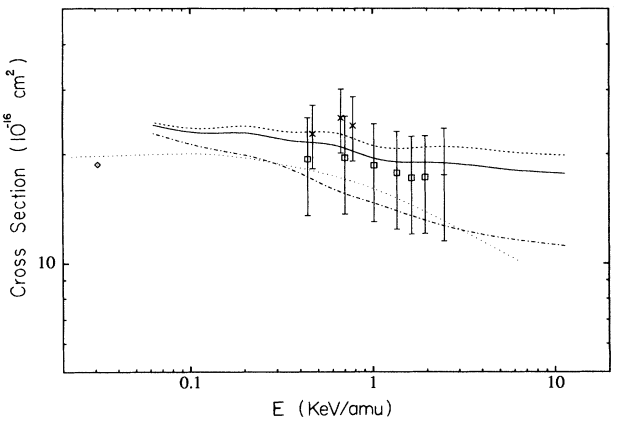

FIG. 3. Cross sections for the single-electron-capture process. The calculated results with Σ and Π states and with only Σ states for the triplet manifold are presented by broken and dotted curves, respectively. The chain curve is the calculated results for the singlet manifold. The full curve represents the statistical weighted sums of the triplet and singlet manifolds. Measurements are also shown: +, Ref. [3]; ×, Ref. [4]; □, Ref. [6].

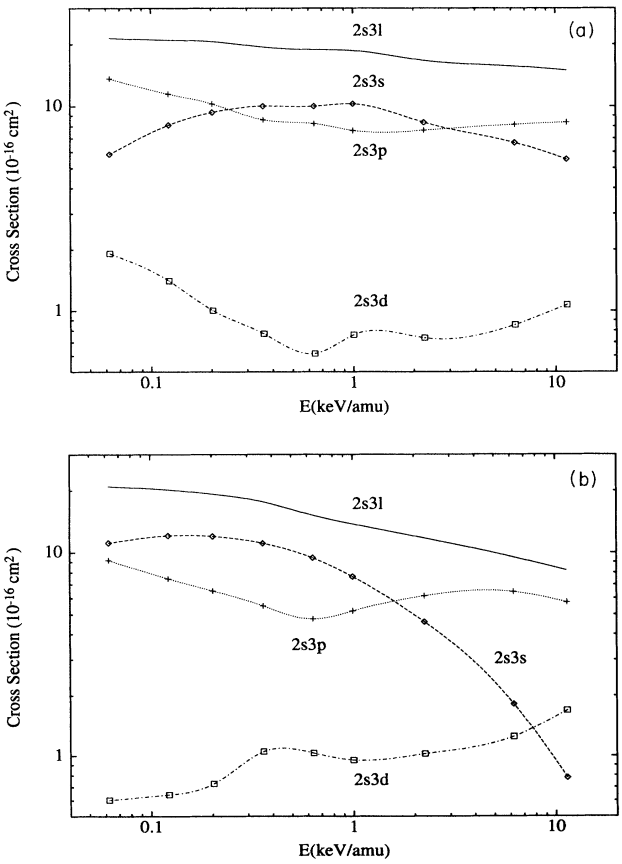

FIG. 4. Partial cross sections for the one-electron-capture process for the (a) triplet and (b) singlet manifolds, respectively, as a function of energy.

most dominant and compete with each other in both formations. Capture into the $O^{4+}(2s3d)$ state is smaller by about an order of magnitude than those two processes. For the singlet formation, the $O^{4+}(2s3p)$ is relatively smaller than in the triplet formation at intermediate collision energies. Kimura *et al.* [5] measured n and l distributions of captured electrons and suggested that at $E=0.326$ keV/u the $O^{4+}(2s3l)$ states are selectively populated, and among them $O^{4+}(2s3s)$ and $O^{4+}(2s3p)$ are dominant and the $O^{4+}(2s3d)$ state is by far the smallest. Our present result is found to be consistent with this experimental finding.

4. *Partial distributions of the RTE process*

a. Triplet. In Fig. 5(a), the partial cross sections of the RTE process are displayed for the triplet formation. The capture into the $O^{4+}(2p3s\ ^3S)$ state occurs dominantly over the entire energy region studied, followed by the $O^{4+}(2p3p\ ^3P)$. At the lower collision energies, the cross sections of the $O^{4+}(2p3d\ ^3D)$ and $O^{4+}(2p3d\ ^3P)$ states become comparable to $O^{4+}(2p3p\ ^3P)$. The time dependence of the transition probability (not shown) indicates that the transition to these states occurs through the SEC channels at intermediate distances, i.e., the direct transition from the initial channel to these RTE channels at large internuclear distance is not effective in this system. The flux, which finally reaches into the RTE channels from the SEC channels and, successively from the PE channel, is distributed among many RTE channels on the outgoing trajectory of the collision. The energy splitting between the 5Σ and 6Σ states at R_7 and its location are effective for the transition (within the reaction window) and, hence, the flux flow into the $O^{4+}(2p3s)+He^+$ channel effectively proceeds. The Auger threshold channel is $O^{4+}(3l3l')$ and hence, RTE states studied here, viz. $O^{4+}(2p3l)$, do not decay through the Auger process.

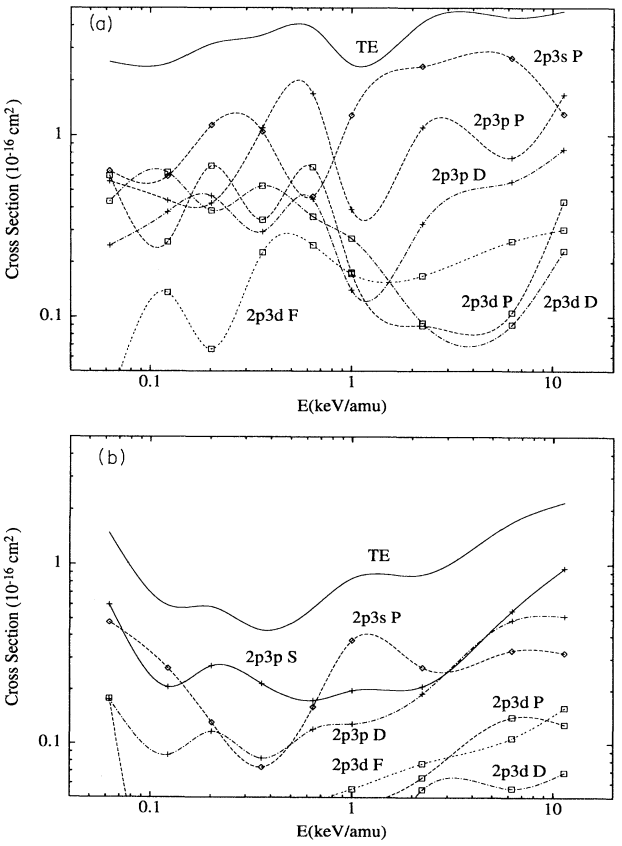

FIG. 5. Partial cross sections for the transfer-excitation process for the (a) triplet and (b) singlet manifolds, respectively, as a function of energy.

b. Singlet. The partial cross sections of the RTE for the singlet formation are displayed in Fig. 5(b). Comparison of this figure to the triplet formation shows that all the cross sections in the singlet are smaller (before the statistical consideration). This is because the transition from PE to RTE channels at the avoided crossing R_7 and larger internuclear distance is somewhat less efficient due to increasing diabaticity for the singlet (see the difference in energy splittings in Table I). Among those, the cross sections of the $O^{4+}(2p3p\ ^1S)$, $O^{4+}(2p3s\ ^1P)$, and $O^{4+}(2p3p\ ^1D)$ states are relatively larger than the rest. This is because the combination of the energy splittings at each corresponding avoided crossing and their couplings are optimal to these states within the present collision energies, making the transition favorable. Consequently, these states play the role of a reservoir in the redistribution of the flux within the RTE channels.

C. Target ionization and projectile loss processes

Some results on ionization mechanisms through a test calculation with inclusion of discretized continua that correspond to target ionization and projectile loss will be discussed here to some extent. Three sets of test calculations were carried out by including (a) target ionization channels ($1d$) *only*, including (i) all couplings within this set and (ii) couplings that directly connect between the initial and target ionization; (b) projectile loss ($1e$) *only*, including (i) all couplings in this set and (ii) couplings that connect the initial channel and projectile ionization; and (c) both target-ionization and projectile-loss channels with all couplings with discrete channels at 1 and 10 keV/u. [Note that we neglected all couplings among continua. Further, in all calculations, a number of original discrete-basis states included, described earlier, is reduced to one-half by selecting dominant contributors in each group of substates while some higher states corresponding to $O^{4+}(2s5l)$ are added.] The basis sets (i) and (ii) both for the (a) target and (b) projectile are specifically intended to help us understand the coupling scheme and ionization mechanism for target ionization and projectile loss by turning on and off the effect of the initial and PE channels. This study also provides, to some degree, the contribution of direct-impact ionization (the result obtained by dropping couplings between target ionization and the initial channels). The third set (c) is for all ionization effects and examines a relative convergence of ionization.

The present magnitude of the ionization cross section constitutes only 0.3% of the total single-electron-capture cross section at 1 keV/u, although this fraction some-

what increases at 10 keV/u. This value of the ratio is consistent with that of 1.3% obtained by the CTMC [16] at 50 keV, and hence ionization is considered to be still a minor process in the present energy range. The ratio of the result based on set (a) [(i)] to that for (c) is more than 90% for both energies studied, implying the importance of target ionization rather than projectile loss. This may be due to the fact that the energy defect between the two asymptotic eigenenergies for the single capture ($O^{4+}+He^{+}$) and target ionization ($O^{5+}+He^{+}+1e$) channels is smaller than that between the projectile-loss ($O^{6+}+He+1e$) and single-capture channels, which allows a stronger perturbation for the electron distribution, hence leading to a larger ionization in target ionization. The large disparity between the two binding energies (24.6 eV vs 138 eV for the He and O^{5+}, respectively) also contributes to ionization and electron loss in this collision energy domain.

Our fraction of the target ionization to direct-impact ionization, i.e., $f=\sigma^{TI}/(\sigma^{TI}+\sigma^{DI})$, is approximately 97%, suggesting the importance of the ladder-climbing mechanism of ionization, or molecular mechanism, over direct-impact ionization in the present energy region. This observation is consistent with our view that all discrete processes are found to proceed on the outgoing part of the collision after single-electron capture is completed, the first step for the ladder climbing. Then, the transferred electron subsequently undergoes a series of excitations within the projectile. An analysis of the ejected electron-energy distribution seems to suggest that the energy of the ionized electron concentrates within a narrow band near zero energy. This finding also supports our finding of the dominance of the ladder-climbing mechanism for target ionization, in which the bound electron gains a small amount of energy, undergoes a series of excitations, and eventually escapes from the molecular field, carrying a small fraction of impact energy. Although these arguments are based on a small-scale study and are considered to be still tentative, we feel, nevertheless, that the essential underlying physics are correctly represented.

D. Projectile excitation

Projectile excitation along with total RTE and SEC are illustrated in Fig. 6. The PE closely relates to the RTE. The cross sections for the RTE and PE show slight out-of-phase oscillatory structures due to strong couplings between two sets of channels. The PE is also out of phase with the SEC for $O^{4+}(2s4l)$ for the same reason as that for the RTE. As described above in Sec I, two pathways are possible for the PE, namely, (i) a target electron is captured into an excited orbital in the projectile earlier in the collision and, at a later time, an inner electron is transferred back to the target; or (ii) a single direct excitation of the projectile electron occurs. Our study indicates that it is likely to proceed through the process (i), resulting in the PE. This observation may be somewhat surprising because process (i) is the two-step process. However, single-capture processes take place dominantly

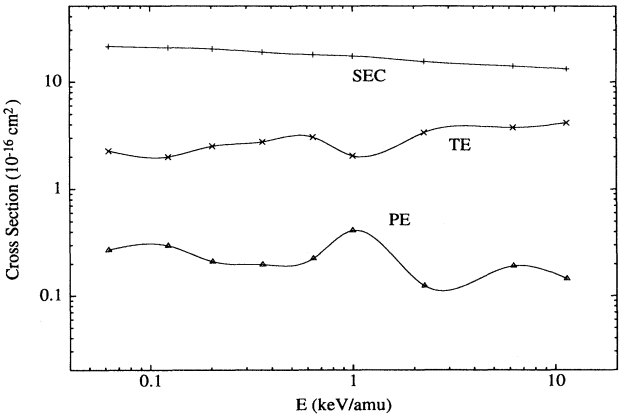

FIG. 6. Cross sections for the projectile excitation (PE) along with total SEC and RTE.

at an earlier time in the collision, and this two-step process follows naturally. Of course, the direct PE (ii) is possible, particularly for large impact parameters, but its magnitude is considered to be generally small. As two particles approach closer, the flux is well mixed, i.e., a molecular effect, leaving most of it in two-electron processes, which is favorable to the mechanism (i).

IV. SUMMARY OF CONCLUSIONS

The theoretical study of electron capture resulting from collisions of O^{5+} ions with He atoms has been carried out by applying a semiclassical molecular-orbital expansion method in the energy range from 62.5 eV/u to 11.3 keV/u. Total cross sections gently decrease with the collision energy and are in good accord with measurements. At all the collision energies studied, the single-electron-capture process is dominant and transfer excitation and projectile excitation follow. All processes are found to occur after transitions from the initial channel to the single-electron-capture channels completed at first in the incoming part of the collision, therefore reducing direct PE and RTE contributions to the dynamics.

ACKNOWLEDGMENTS

This work was supported by the U.S. Department of Energy, Office of Energy Research, Office of Health and Environmental Research, under Contract No. W-31-109-Eng-38 (M.K.); by the Office of Basic Energy Sciences, Division of Chemical Sciences, through Rice University (N.S.); and by the R. A. Welch Foundation (N.S.). N.S. was also supported by a Grant-in-Aid for Scientific Research on Priority Areas, Atomic Physics of Multicharged Ions (Area No. 239/05 238 204), and Molecular Magnetism (Area No. 228/05 226 215), from the Ministry of Education of Japan (01 540 312). Some portions of the present calculation were carried out at the computer centers of Tohoku University and Niigata University.

[1] N. Shimakura, H. Sato, M. Kimura, and T. Watanabe, J. Phys. B **20**, 1801 (1987).
[2] N. Shimakura, S. Suzuki, and M. Kimura, Phys. Rev. A **48**, 3652 (1993).
[3] L. D. Garnder, J. E. Bayfield, P. M. Koch, I. A. Sellin, D. J. Pegg, R. S. Peterson, M. L. Mallory, and D. H. Crandall, Phys. Rev. A **20**, 766 (1979).
[4] T. Iwai, Y. Kaneko, M. Kimura, N. Kobayashi, S. Ohtani, K. Okuno, S. Takagi, H. Tawara, and S. Tsurubuchi, Phys. Rev. A **26**, 105 (1982).
[5] M. Kimura, T. Iwai, Y. Kaneko, N. Kobayashi, A. Matsumoto, S. Ohtani, K. Okuno, S. Takagi, H. Tawara, and S. Tsurubuchi, J. Phys. B **15**, L851 (1982).
[6] R. Hoekstra, F. J. de Heer, and H. Winter, Nucl. Instrum. Methods Phys. Res. Sect. B **23**, 104 (1987).
[7] W. Waggoner, C. L. Cocke, L. N. Tunnell, C. C. Havener, F. W. Meyer, and R. A. Phaneuf, Phys. Rev. A **37**, 2386 (1988).
[8] J. P. Bangsgaard, P. Hvelplund, J. O. P. Pedersen, L. R. Andersson, and A. Barany, Phys. Scr. **T28**, 91 (1989).
[9] J. R. MacDonald and F. W. Martin, Phys. Rev. A **4**, 1965 (1971).
[10] H. Knudsen, H. K. Haugen, and P. Hvelplund, Phys. Rev. A **23**, 597 (1981).
[11] J. E. Bayfield, L. D. Gardner, Y. Z. Gulkok, T. K. Saylor, and S. D. Sharma, Rev. Sci. Instrum. **51**, 651 (1980).
[12] S. A. Boman, E. M. Bernstein, and J. A. Tanis, Phys. Rev. A **39**, 4423 (1989).
[13] J. A. Tanis, M. W. Clark, R. Price, and R. E. Olson, Phys. Rev. A **36**, 1952 (1987).
[14] J. K. Swenson, Y. Yamazaki, P. D. Miller, H. F. Krause, P. F. Dittner, P. L. Pepmiller, S. Datz, and N. Stolterfoht, Phys. Rev. Lett. **57**, 3042 (1986).
[15] T. J. M. Zouros, D. H. Lee, and P. Richard, Phys. Rev. Lett. **62**, 2261 (1989).
[16] R. K. Janev and M. R. C. McDowell, Phys. Lett. **102A**, 405 (1984).
[17] M. Kimura and N. F. Lane, in *Advances in Atomic, Molecular, and Optical Physics,* edited by D. R. Bates and B. Bederson (Academic, New York, 1989), Vol. 26, p. 79.
[18] M. Kimura, H. Sato, and R. E. Olson, Phys. Rev. A **28**, 2085 (1983).
[19] A. Dalgarno, Adv. Phys. **22**, 281 (1962).
[20] A. M. Ermolaev, J. Phys. B **25**, 3133 (1992).
[21] A. Jain, C. D. Lin, and W. Fritsch, Phys. Rev. A **34**, 3676 (1986).
[22] L. Opradolce, P. Valiron, and R. McCarroll, J. Phys. B **16**, 2017 (1983).
[23] S. Bashkin and J. R. Stoner, Jr., *Atomic Energy Levels and Grotorian Diagrams I* (North-Holland, Amsterdam, 1975).
[24] M. Kimura and N. F. Lane, Phys. Rev. A **41**, 5938 (1990).